Transfer matrix spectrum of two-dimensional layered Ising models

1991 J. Phys. A: Math. Gen. 24 5121

(http://iopscience.iop.org/0305-4470/24/21/023)

J. Phys. A: Math. Gen. **24** (1991) 5121–5136. Printed in the UK

Transfer matrix spectrum of two-dimensional layered Ising models*

Laurent Frachebourg† and Malte Henkel†‡

† Département de Physique Théorique, Université de Genève, 24 quai Ernest Ansermet, CH-1211 Genève 4, Switzerland

‡ HLRZ, KFA Jülich, Postfach 1913, D-5170 Jülich, Federal Republic of Germany

Received 2 April 1991, in final form 4 June 1991

Abstract. A class of layered Ising models interpolating between the homogeneous Ising model and the McCoy–Wu model is studied. Critical exponents and the transfer matrix spectrum at the critical point are calculated numerically using finite-size scaling techniques and analytically by using an analogy with an electron gas in a crystal with impurities. The transfer matrix spectrum is compared with those of some strongly anisotropic critical systems.

1. Introduction

Since nature seems simple, but is not simplistic, these have always been attempts to understand complicated systems in terms of the simplest possible model. The 2D Ising model is the simplest model of ferromagnetism which shows a non-trivial critical behaviour and still admits an exact solution. To go beyond the idealization of homogeneous models, McCoy and Wu [1, 2] proposed a layered Ising model and showed by exact solution that this modified system indeed displays a different critical behaviour. Here, we are considering a generalization of this model, as described by the action S (also referred to as classical Hamiltonian $\mathcal{H}$) [3]

$$S = -J_1 \sum_{p=1}^{n\mathcal{M}+1} \sum_{q=-\mathcal{N}+1}^{\mathcal{N}} \sigma_{p,q}\sigma_{p,q+1} - \sum_{p=0}^{\mathcal{M}-1} \sum_{l=1}^{n} \sum_{q=-\mathcal{N}+1}^{\mathcal{N}} J_2(l)\sigma_{np+l,q}\sigma_{np+l+1,q} \tag{1.1}$$

where the σ are classical Ising spins and J_1 and $J_2(l)$ are coupling constants, where $J_2(l)$ describes the inhomogeneity. The longitudinal extent of the lattice is $2\mathcal{N}$ in the non-modified direction and $\mathcal{N} = n\mathcal{M}$ in the transverse one. One can consider the action (1.1) as the homogeneous one but modified with defect lines as described by the $J_2(l)$. One would like to calculate the thermodynamics in the limit of large lattices. In particular, the following choices can be studied.

1. Take the limits $\mathcal{M}, \mathcal{N} \to \infty$, but keep n finite. This case corresponds to the model originally studied in [1], considering the $J_2(l)$ as independent random variables with probability distribution function $P(J_2)$. It was found that if $P(J_2)$ is sharply peaked then the specific heat has an infinitely differentiable essential singularity at the critical point [1]. Later studies further investigated the specific heat as a function of n and showed that if n becomes large, the specific heat amplitude as obtained for the

* Supported in part by the Swiss National Science Foundation.

0305-4470/91/215121+16$03.50

homogeneous Ising model is strongly suppressed [3]. The concept of frustration plaquettes has been very useful in analysing in detail the thermodynamic behaviour [4, 5]. Excitation spectra of related Ising models were also studied recently [6].

2. Let $\mathcal{N} \to \infty$, but keep $\mathcal{M}$ finite. Then the distance of the defect lines $n = N/\mathcal{M}$ will scale with the transverse size N of the lattice. This case did receive a lot of attention recently, both at the critical point and in the non-critical regime. It was first studied for $\mathcal{M} = 2$, where it was shown that the exponents of the local magnetization and of the local correlation functions depend continuously on the J_2 [7, 8]. For $\mathcal{M} = 1$, this is merely a modified boundary condition [9–12]. Although these boundary conditions are not invariant under the whole set of 2D conformal transformations, the well known relationship [13] of the finite-size scaling amplitudes of the correlation length and critical exponents remains valid [14]. The critical exponents thus obtained are generalizations of the familiar surface (or corner) exponents. The critical correlation length spectrum has been investigated in much detail [15–20]. In particular, it was shown that for any finite number $\mathcal{M}$ of defect lines, the model is conformally invariant if and only if the spacings of the defect lines are commensurate with each other [20]. In this case, the spectrum can be obtained from the unitary irreducible representations of a $O(2\mathcal{M})$ Kac–Moody algebra [19–21] and the conformal central charge is $c = \mathcal{M}$ for almost all values of the couplings J_2, as compared with $c = 1/2$ for the homogeneous model. For commensurate defect spacings, the inhomogeneity introduced by the defect lines breaks the conformal group $V \otimes V$ to their diagonal subgroup, as can be seen by explicit construction of the generators [18]. These results also hold for the case of extended layers [22]. Line defects have also been studied in a more general defect geometry [23], as well as for generalized defect couplings [24].

Another possibility is to keep $\mathcal{M} = 1$, but to consider extended defects close to the surface [25, 26]. These extended defect perturbations can be relevant, marginal or irrelevant, depending on how fast $J_2(l)$ approaches its bulk value. If the perturbation is marginal, the preservation of conformal invariance depends on the detailed profile of $J_2(l)$. Surprisingly, numerical and analytical studies suggest that the correlation length amplitude–exponent relation stays intact, even if the spectrum can no longer be cast into irreducible representations of the conformal group [27–29]. Radial extended defects have also been studied [30, 31].

We want to consider an interpolation between the two cases mentioned. We let both n and $\mathcal{M}$ become large (the limit $\mathcal{N} \to \infty$ is understood) but impose the condition

$$n = N/\mathcal{M} = aN^{\theta} \tag{1.2}$$

such that in each strip of width n there is only one defect line and where $0 < \theta < 1$ and a are constants. The cases $\theta = 0$ and $\theta = 1$ correspond to the situations already mentioned. For simplicity, we take $J_1 = J_2 = J_c$ away from the defect lines and choose the *defect strength* $\kappa = J_{2,\text{defect}}/J_{2,\text{no defect}}$ to be the same for all defect lines. The defect configuration is sketched in figure 1. Systems of this kind (with an additional averaging done over the defect couplings) were studied using ε-expansion techniques [32].

We shall be interested in calculating the transfer matrix spectrum at the critical point. For conformally invariant systems, the complete operator content (*all* relevant, marginal and irrelevant scaling fields) can be read from the transfer matrix spectrum [33, 34]. Although our model is not conformally invariant (see below), the transfer matrix spectrum might still contain important information.

Consider for a moment the case $\kappa = 0$. Then the model decomposes into $\mathcal{M}$ independent systems, each of size n, with free boundary conditions. The correlation length

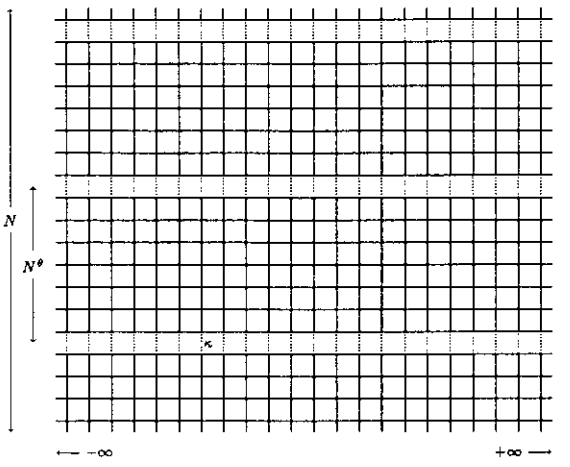

Figure 1. The 2D strip geometry with the defect lines. The coupling J_1, J_2 is normalized to one away from the defects and κ is the defect strength.

along the strip is then obtained from conformal invariance [13, 33]

$$\xi_\parallel = \frac{1}{\pi x(0)}\, n = \frac{a}{\pi x(0)}\, N^\theta \qquad \kappa = 0 \tag{1.3}$$

where $x(0)$ is a surface critical exponent of the usual 2D Ising model. On the other hand, for $\kappa = 1$ we have $\xi_\parallel = N/(2\pi x(1))$ with $x(1)$ a bulk critical exponent. The line defect perturbation has an RG eigenvalue exponent $y_\kappa = 2 - \theta - x_\varepsilon$. For $\theta < 1$, the defect perturbation is relevant close to $\kappa = 1$ in the 2D Ising model ($x_\varepsilon(\kappa = 1) = 1$) and irrelevant close to $\kappa = 0 (x_\varepsilon(\kappa = 0) = 2)$ and we expect

$$\xi_\parallel \sim N^\theta \qquad \kappa \neq 1 \tag{1.4}$$

(see also [32]). Such a behaviour, for $\theta \neq 1$, is not consistent with conformal invariance, but is rather characteristic of directed (or dynamical) systems, where the exponent θ is related to the two correlation length exponents $\nu_\perp$, $\nu_\parallel$:

$$\theta = \nu_\parallel / \nu_\perp . \tag{1.5}$$

The transfer matrix spectrum of directed percolation and of the tight-binding model has been studied recently [35]. Surprisingly, it was found that the transfer matrix spectra are very similar, although the models are in different universality classes.

The layered Ising model we are going to study has the advantage that it shares with true directed systems the feature that the anisotropy of the model is relevant and leads to two different exponents $\nu_\perp$ and $\nu_\parallel$. (In higher dimensions, ε-expansion techniques suggest a similar anisotropic scaling [32].) The exponent θ can be chosen differently from the mean-field value $\theta = 2$ and the model still remains exactly solvable. In the absence of a general theory, the objective of this paper is to obtain further insight into the phenomenology, in particular in low dimensions, by studying another simple example.

In fact, we prefer for technical reasons to consider the quantum Hamiltonian H of the classical action S, as defined by the transfer matrix $\mathcal{T} = \exp(-\tau H)$. In the extreme

anisotropic limit $J_1 \to 0$, $J_2 \to \infty$ with $J_1 \exp(+2J_2)$ being fixed, the Hamiltonian takes a simple form for $\tau \to 0$ (which automatically guarantees $\mathcal{N} \to \infty$)

$$H = -\tfrac{1}{2} \sum_{k=1}^{N} [t\sigma^z(k) + \sigma^x(k)\sigma^x(k+1)] - \tfrac{1}{2}(\kappa - 1) \sum_{k}{}' \sigma^x(k)\sigma^x(k+1) \tag{1.6}$$

where the σ are Pauli matrices, t corresponds to the temperature and the prime on the second sum indicates that the defects are placed such that (1.2) is satisfied. Periodic boundary conditions are implied. Since the density of the defects $\mathcal{M}/N \sim N^{-\theta} \to 0$ for $N \to \infty$, it follows that the critical point $t_c = 1$ is the same as for the defectless system. Although we are treating here exclusively the case of (thin) line defects, our results should translate directly to the case of thick layers, as shown for $\mathcal{M}$ finite [22].

The correspondence of the eigenvalues E_i of H with the thermodynamics determined by the action S is well known (for a review, see [34]). The correlation lengths $\xi_{\parallel,i}$ of the local fields and the free energy per spin f are obtained from

$$\xi_{\parallel,i}^{-1} = E_i - E_0 \qquad f = E_0/N \tag{1.7}$$

where E_0 is the ground state energy of H. Although we are studying an anisotropic system, taking the Hamiltonian limit leading to H is allowed, at least if the global symmetry is unaffected. This can be checked for genuinely anisotropic systems like directed percolation, where the universality of the critical exponents was explicitly confirmed [35, 36]. We therefore expect that our results will immediately translate to the isotropic transfer matrix by universality [34].

The contents of this paper are as follows. In section 2, the spectrum of H is studied numerically. We shall give evidence that the relationship (1.5) is indeed satisfied and we calculate $\nu_\parallel$ and $\nu_\perp$. Since H can be written in terms of fermionic harmonic oscillators, its entire spectrum is determined by the energies of the one-particle excitations. Our numerical analysis allows us to guess the form of these, as specified in (2.12) and (2.13). Some tests on the universality of the spectrum are also performed. Section 3 gives the analytic solution for the spectrum and confirms the results of the numerical analysis. This will be done by using an analogy to an electron gas. Section 4 gives our conclusions.

2. Numerical finite-size scaling calculation

In this section, we calculate the eigenvalues of the quantum Hamiltonian H numerically, using finite-size scaling techniques. The comparison with the analytical results, to be obtained in section 3, allows an assessment of the reliability of the numerical methods for a non-isotropic critical point, while previous studies have up to now mainly concentrated on isotropic systems [34]. The technique employed diagonalizes H on finite chains of N sites and then extrapolates for $N \to \infty$. We shall use the BST extrapolation algorithm [37, 38] for that purpose. For detailed reviews on extrapolation techniques, see [39, 40].

2.1. General remarks

The diagonalization of H follows the familiar technique of Lieb, Schultz and Mattis [41]. We begin by rewriting the Hamiltonian H in terms of fermionic operators $c(m)$

by a Jordan-Wigner transformation

$$H=\sum_{m=1}^{N} t[c^{\dagger}(m)c(m)-\tfrac{1}{2}]-\tfrac{1}{2}\sum_{m=1}^{N-1}[(c^{\dagger}(m)-c(m))(c^{\dagger}(m+1)+c(m+1))]$$
$$+(\tfrac{1}{2}-Q)(c^{\dagger}(N)-c(N))(c^{\dagger}(1)+c(1))$$
$$+\tfrac{1}{2}(1-\kappa)\sum_{j}(c^{\dagger}(N_j)-c(N_j))(c\dagger(N_j+1)+c(N_j+1)) \tag{2.1}$$

$$=\sum_{n,m=1}^{N}[c^{\dagger}(n)\mathbf{A}_{nm}c(m)+\tfrac{1}{2}(c^{\dagger}(n)\mathbf{B}_{nm}c^{\dagger}(m)+\text{HC})]+\text{constant} \tag{2.2}$$

where κ is the defect strength, $\mathbf{A}$ is a symmetric and $\mathbf{B}$ an antisymmetric matrix and the defects are at the sites N_j such that their distance is $n=aN^{\theta}$. The operator

$$Q=\frac{1}{2}\left[1-\exp\left(i\pi\sum_{m=1}^{N}c^{\dagger}(m)c(m)\right)\right] \tag{2.3}$$

commutes with H and divides its spectrum into the two sectors $Q=0$, 1 which correspond to an even or odd number of excited fermionic states, respectively. Now, H can be written in diagonal form

$$H=\sum_{k}\Lambda(k)(\eta_k^{\dagger}\eta_k-\tfrac{1}{2}) \tag{2.4}$$

where the eigenvalues $\Lambda(k)$ are determined from

$$\mathbf{M}\psi_k=(\mathbf{A}-\mathbf{B})(\mathbf{A}+\mathbf{B})\psi_k=\Lambda(k)^2\psi_k \tag{2.5}$$

where $\mathbf{M}$ is the following $N\times N$ matrix (we have taken $t=1$):

$$\mathbf{M}=\begin{pmatrix} 2 & -1 & & & & & & & (1-2Q) \\ -1 & 2 & -1 & & & & & & \\ & & \cdots & & & & & & \\ & & & 2 & -1 & & & & \\ & & & -1 & 1+\kappa^2 & -\kappa & & & \\ & & & & -\kappa & 2 & -1 & & \\ & & & & & \cdots & & & \\ & & & & & & & 2 & -1 \\ (1-2Q) & & & & & & & -1 & 2 \end{pmatrix} \tag{2.6}$$

Note that the eigenvalues $\Lambda(k)$ depend explicitly on the sector Q. This is the starting point for the analytical solution in section 3.

For the numerical calculations, we proceed as follows. Consider $\theta=p/q$, $p\leqslant q$. Choose the length N of the quantum chain such that $N=(2l)^q$, where $l=1,2,\ldots$ is a positive integer. The number of defects is $\mathcal{M}=(2l)^{q-p}$ and the defects, all having the same defect strength κ, are equidistantly distributed at a distance $n=(2l)^p$. We now proceed to diagonalize M.

2.2. Correlation lengths

We first check the critical point finite-size scaling. Consider the spin-spin correlation length

$$\xi_{\parallel}^{-1}=E_1-E_0\sim N^{-\tilde{\theta}}. \tag{2.7}$$

Finite-size estimates for $\tilde{\theta}$ are obtained from [42]

$$\frac{\ln(\xi_{\parallel,N}(t_c)/\xi_{\parallel,N'}(t_c))}{\ln(N/N')} = \tilde{\theta} \tag{2.8}$$

where we have used that the critical point is at $t = t_c = 1$. In tables 1 and 2, we give numerical estimates as obtained for some values of θ and κ. We see that indeed $\tilde{\theta} = \theta$, as expected.

Next, we obtain an estimate for the exponent $\nu_\perp$ from [42]

$$\zeta = \frac{\ln((\partial/\partial t)\xi_{\parallel,N}/(\partial/\partial t)\xi_{\parallel,N'})}{\ln N/N'} = \frac{1}{\nu_\perp} + \theta. \tag{2.9}$$

In tables 1 and 2, we give estimates for the exponent ζ as obtained for $\kappa = 1/2$. The results are consistent with $\nu_\perp = 1/\theta$ which implies $\nu_\parallel = 1$, independent of θ. This means that the inhomogeneity introduced by the defects is not strong enough to change the correlation length scaling in this direction. This is not surprising, since the density of defects $\mathcal{M}/N$ still vanishes in the $N \to \infty$ limit, provided $\theta > 0$. Summarizing, we have,

Table 1. Finite-size estimates for the exponents $\tilde{\theta}$ and ζ as defined in the text, for several lattices of size N. The data were obtained for $\theta = 1/2$. The line denoted by ∞ gives the extrapolated values as obtained with the BST extrapolation algorithm and the numbers in brackets give the estimated uncertainty in the last given digit(s).

	$\kappa = 0.5$		$\kappa = 0.2$	$\kappa = 0.8$
N	$\tilde{\theta}$	ζ	$\tilde{\theta}$	$\tilde{\theta}$
36	0.437 3092	0.8107	0.455 7964	0.007 1921
64	0.470 3935	0.9072	0.468 5289	0.266 6158
100	0.481 5034	0.9475	0.475 3470	0.362 7573
144	0.486 1502	0.9647	0.479 7125	0.413 1473
196	0.488 6170	0.9722	0.482 7585	0.443 1416
256	0.490 2084	0.9774	0.485 0068	0.462 0401
324	0.491 3663	0.9797	0.486 7351	0.474 2829
400	0.492 2660	0.9821	0.488 1054	0.482 3300
484	0.492 9922	0.9838	0.489 2187	0.487 6644
576	0.493 5921	0.9851	0.490 1413	0.491 2206
676	0.494 0971	0.9861	0.490 9182	0.493 6044
784	0.494 5292		0.491 5816	0.495 2120
900	0.494 9004		0.492 1542	0.496 3016
1024	0.495 2256		0.492 6542	0.497 0454
1156	0.495 5120		0.493 0940	0.497 5600
1296	0.495 7650		0.493 0940	0.497 9318
1444	0.495 9936		0.493 8318	0.498 1994
1600	0.496 1926		0.494 1457	0.498 3712
1764	0.496 3797		0.494 4290	0.498 5063
1936	0.496 5439		0.494 6886	0.498 6292
2116	0.496 7047		0.494 9156	0.498 7799
2304	0.496 8316		0.495 1339	0.498 8038
2500	0.496 9788		0.495 3313	0.498 8162
∞	0.500 0 (1)	0.995 (10)	0.500 (1)	0.50 (1)
expected	$\frac{1}{2}$	1	$\frac{1}{2}$	$\frac{1}{2}$

Table 2. Finite-size estimates for the exponents $\tilde{\theta}$ and ζ, obtained for $\kappa = 1/2$. The line denoted by ∞ contains the extrapolated values from the BST algorithm and the numbers in brackets give the estimated uncertainty in the last given digit.

	$\theta = 1/3$		$\theta = 2/3$	
N	$\tilde{\theta}$	ζ	$\tilde{\theta}$	ζ
64	0.285 3013	0.5327	0.541 8697	1.0272
216	0.314 4492	0.6231	0.635 4485	1.2288
512	0.319 7045	0.6352	0.656 3818	1.2917
1000	0.322 6500	0.6418	0.662 5136	1.3152
1728	0.324 5423	0.6460	0.664 5552	1.3268
2744	0.325 8625	0.6490	0.665 3573	1.3296
∞	0.3333 (4)	0.666 (1)	0.666 (5)	1.34 (1)
expected	$\frac{1}{3}$	$\frac{2}{3}$	$\frac{2}{3}$	$\frac{4}{3}$

independently of $\kappa(\neq 1)$:

$$\nu_\perp = \frac{1}{\theta} \qquad \nu_\parallel = 1. \tag{2.10}$$

For a discussion of the scaling of the free energy, see below.

We now discuss the excitation spectrum of H. Since $\xi \sim N^\theta$, we consider the finite-size scaling amplitudes of the one-fermion states

$$A_i^{(Q)} = \frac{\Lambda_i^{(Q)} N^\theta}{\pi} \tag{2.11}$$

which depend on the eigenvalues of Q. The normalization of the $A_i^{(Q)}$ is motivated from the case $\kappa = 0$. In figures 2 and 3, we show finite-size estimates for the amplitudes $A_i^{(0)}$, $A_i^{(1)}$. A band structure for the one-particle states is apparent.

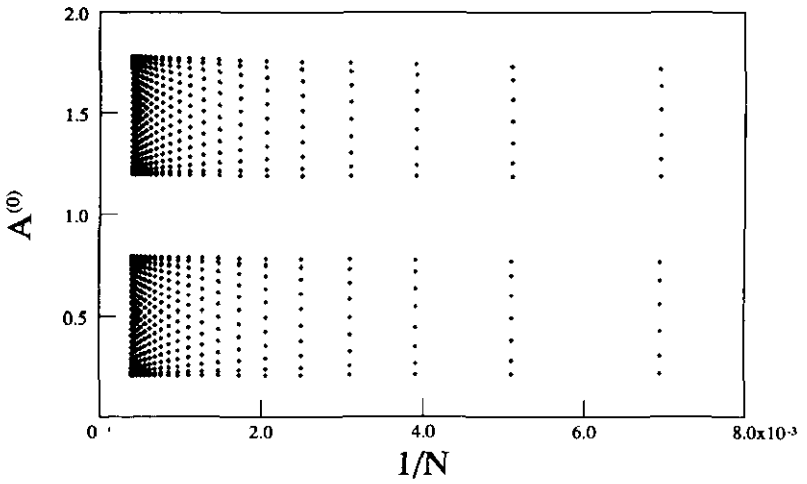

Figure 2. Spectrum of the finite-size scaling amplitudes $A^{(0)}$ of the one-fermion levels of H for $\theta = 1/2$ and $\kappa = 1/2$ in the sector $Q = 0$.

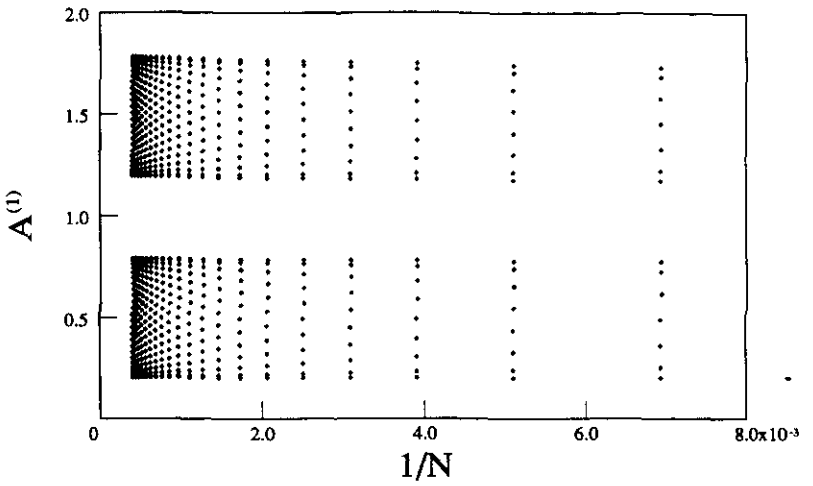

Figure 3. Spectrum of the finite-size scaling amplitudes $A^{(1)}$ of the one-fermion levels of H for $\theta = 1/2$ and $\kappa = 1/2$ in the sector $Q = 1$.

For a quantitative description, we parametrize the amplitudes $A_i^{(Q)}$ as follows. For $Q = 0$, we have

$$A^{(0)}(r, m) = \tfrac{1}{2} + r \pm [\Delta(\kappa) - m(m+1)U(\kappa)/N^{2-2\theta}] \tag{2.12}$$

with $r = 0, 1, \ldots, N^{\theta} - 1$; $m = 0, 1, \ldots, \frac{1}{4}N^{1-\theta} - 1$. In writing this, we tacitly assume that m is a small integer. Otherwise, the higher-order terms in $1/N$ neglected here must be taken into account (see section 3). All one-particle amplitudes $A^{(0)}$ are twofold degenerate.

For $Q = 1$, we have

$$A^{(1)}(r, m) = \tfrac{1}{2} + r \pm [\Delta(\kappa) - m^2 U(\kappa)/N^{2-2\theta}] \tag{2.13}$$

with the same values of r and m as above. Besides the value $m = 0$, where the corresponding amplitudes are non-degenerate, all other $A^{(1)}$ are twofold degenerate.

Note that $\Delta(\kappa)$ and $U(\kappa)$ are the same for both values of Q and are given by

$$\Delta(\kappa) = 1 - \frac{2}{\pi}\tan^{-1} 1/\kappa = \frac{1}{2} - \frac{1}{\pi}\cos^{-1}\frac{2\kappa}{1+\kappa^2} \tag{2.14}$$

$$U(\kappa) = \frac{4\pi\kappa}{1-\kappa^2}. \tag{2.15}$$

As they stand, (2.14) and (2.15) are only valid for $0 \leqslant \kappa < 1$. For other values of κ, one has to choose the appropriate branch of the $\tan^{-1}$. In table 3, we give some numerical estimates for the functions $\Delta(\kappa)$ and $U(\kappa)$. Our numerical results are in agreement with the above equations. The equations (2.11)–(2.15) give the exact solution for the *entire* spectrum of H. We shall prove them in section 3.

We note the following.

1. The one-particle states fall into broad energy bands. This is described by the two quantum numbers r and m. r characterizes the different energy bands, while m distinguishes, up to the last twofold degeneracy, the levels inside a given band. The

Table 3. Numerical estimates for the functions $\Delta(\kappa)$ and $U(\kappa)$ describing the scaled one-particle spectrum of the quantum Hamiltonian (1.6) and their comparison with the analytical results.

		Numerical		Analytic	
θ	κ	$\Delta(\kappa)$	$2U(\kappa)$	$\Delta(\kappa)$	$2U(\kappa)$
$\frac{1}{2}$	0.2	0.125 (2)	5.23 (2)	0.125 666	5.2360
	0.5	0.295 15 (10)	16.72 (5)	0.295 167	16.7552
	0.8	0.425 (10)	55.5 (5)	0.429 553	55.8505
$\frac{2}{3}$	0.5	0.295 (1)	16.75 (20)	0.295 167	16.7552
$\frac{1}{3}$	0.5	0.295 15 (20)	16.7 (5)	0.295 167	16.7552

bands are independent of Q and are centred at half-integer values of the $A_i^{(Q)}$. Their width is θ-independent, but depends on κ

$$\Delta A_i^{(Q)} = 2\cos^{-1}\frac{2\kappa}{1+\kappa^2} \tag{2.16}$$

and we recognize the same κ-dependence as for the shifts of the correlation length amplitudes for the single defect line case [18].

2. Inside the bands, the levels are symmetric with respect to the centre. The scaling of the differences of the amplitudes is different from those of the whole bands, as seen in (2.12) and (2.13).

3. In the limit $\theta \to 1$, we retain only the possibility $m = 0$. We then recover the previous results for a single defect line [18].

4. These results were obtained using periodic boundary conditions in (1.6), which implies $Q = 0$ for the Z_2-even and $Q = 1$ for the Z_2-odd states. Antiperiodic boundary conditions are included by simply exchanging the roles of the $Q = 0$ and $Q = 1$ sectors. In particular, this implies that the band structure is independent of the boundary conditions considered here.

It is interesting to observe a different behaviour of the one-particle levels on different scales. On the scale of the whole bands, one has equidistant level spacing, as would have been expected for a conformally invariant system! On the other hand, the excitations inside the bands, which dominate the long-range behaviour of the correlation functions, show a completely different behaviour.

2.3. Ground-state energy

We now discuss the finite-size scaling of the ground-state energy E_0. Its finite-size scaling at the critical point $t = t_c = 1$ is described by the ansatz

$$E_0/N = \sum_{i=0}^{3} B_i N^{-i\theta} + O(N^{-4\theta}) \tag{2.17}$$

which at least for $\kappa = 0$ is certainly correct. We have checked that the form (2.17) stays correct for general κ. In table 4, we give, for $\kappa = 1/2$, numerical estimates for some values of θ. Of course, $B_0 = 2/\pi$ is the bulk term and does not depend on the introduction of the defect lines. Note, however, that the next coefficients also appear to be θ-independent, which gives confidence that the ansatz chosen is meaningful.

Table 4. Finite-size scaling coefficients B_i as defined in (2.18) for the ground-state energy at the critical point for $\kappa = 1/2$ as estimated from the BST algorithm.

θ	B_0	B_1	B_2	B_3
$\frac{1}{3}$	0.636 619 (1)	−0.131 04 (1)	0.03402 (1)	−0.0102 (3)
$\frac{1}{2}$	0.636 61977 (2)	−0.131 041 (5)	0.03400 (2)	−0.0097 (3)
$\frac{2}{3}$	0.636 6197 (1)	−0.131 04 (1)	0.033 (2)	−0.009 (5)

On the other hand, from finite-size scaling theory [43] one would expect that the leading coefficient of the singular free energy should be universal. To check this, we generalize the quantum Hamiltonian (1.6) by including an irrelevant parameter η

$$H = -\frac{1}{2\eta}\sum_{k=1}^{N}\left[t\sigma^z(k)+\tfrac{1}{2}\{(1+\eta)\sigma^x(k)\sigma^x(k+1)+(1-\eta)\sigma^y(k)\sigma^y(k+1)\}\right]$$

$$-\frac{1}{4\eta}(\kappa-1)\sum_{k}'\{(1+\eta)\sigma^x(k)\sigma^x(k+1)+(1-\eta)\sigma^y(k)\sigma^y(k+1)\} \qquad (2.18)$$

and the prime in the second sum indicates that the defects are placed according to (1.2), as described in section 2.1. For the $\kappa = 1$ case, this model was first solved by Katsura [44] and it was shown that for $\eta \neq 0$, the transition at $t = t_c = 1$ stays in the 2D Ising universality class [45]. The introduction of η allows a very transparent test of the universality predictions [43] of finite-size scaling. For $\kappa = 1$, universality is indeed satisfied for the entire correlation length spectrum [46]. Universality was also confirmed for the case of two defect lines [17].

In order to test universality, some care is necessary with the normalization of the Hamiltonian (2.18) if $\theta < 1$. This reflects a certain arbitrariness in taking the Hamiltonian limit leading to (1.6) or (2.18), see [34]. In (2.18), we normalized H according to the case of finitely many defect lines [17]. In fact, we find that a different normalization must be used here. In table 5, we give numerical estimates of the $B_i(\eta, \kappa)$. While the bulk term B_0 can be taken from the homogeneous system [46], the next correction

Table 5. Finite-size scaling coefficients for the ground-state energy for the generalized Hamiltonian (2.19), for $\theta = 1/2$, at the critical point.

η	κ	B_0	B_1	B_2	B_3	B_4
1.0	1.0[a]	$\frac{2}{\pi}$	0	0	0	0.261 799
	1.0	0.636 619 7724	0.0	0.0	0.0	0.261 80 (2)
	0.8	0.636 619 (1)	−0.059 705 (5)	0.007 87 (2)	−0.014 (1)	
	0.5	0.636 619 77 (2)	−0.131 041 (5)	0.034 00 (2)	−0.0097 (3)	
	0.2	0.636 618 7724 (1)	−0.173 2686 (1)	0.059 33 (1)	−0.027 37 (1)	0.015 (1)
	0.0	0.636 618 7724	−0.181 690 114 (1)	0.065 449 (1)	−0.032 724 (2)	
	0.0[a]	$\frac{2}{\pi}$	−0.181 690 113	0.065 449 846	−0.032 724 923	
0.8	0.5	0.745 044 81 (5)	−0.127 357 (1)	0.038 09 (1)	0.0038 (1)	
	0.0	0.745 044 812 (2)	−0.174 135 96	0.065 44 (1)	−0.009 872 (1)	
0.5	0.5	1.088 110 245 (1)	−0.116 455 57 (3)	0.0469 (1)	0.025 37 (1)	
	0.0	1.088 110 245 (5)	−0.153 915 39 (1)	0.065 44 (1)	0.049 21 (1)	
0.2	0.5	2.542 782 (1)	−0.086 054 (5)	0.0619 (1)	0.035 (1)	
	0.0	2.542 78 (1)	−0.1062 (1)	0.065 (1)	0.23 (1)	

[a] Exact results.

might at first sight appear to be η-dependent. In fact, we fail to find any universal coefficient B_i in the finite-size scaling of the free energy. However, if we compare this (see table 6) with the lowest one-particle amplitude $A_1^{(Q)}$ (which is Q-independent), we find a η-independent ratio

$$B_2/A_1 \simeq 0.168(4) \simeq 1/6$$

(for $\kappa = 1/2$, $\theta = 1/2$), which identifies B_2 as the leading singular contribution to the ground-state energy, in agreement with the scaling expectation.

Table 6. Finite-size scaling amplitudes for the lowest gap (A_1) and the ground-state energy (B_2) as a function of the irrelevant parameter η, for $\kappa = 1/2$, $\theta = 1/2$.

η	B_2	A_1	B_2/A_1
1.0	0.034 00 (2)	0.204 88 (1)	0.1660 (1)
0.8	0.038 09 (4)	0.227 030 (5)	0.165 (2)
0.5	0.046 9 (1)	0.277 97 (5)	0.169 (4)
0.2	0.061 9 (1)	0.374 5 (10)	0.167 (3)

Since the line defects represent an irrelevant perturbation close to $\kappa = 0$, we can use the scaling behaviour of the free energy for decoupled strips to get the free energy scaling. On a strip of width N^θ one has for the (singular) free energy density, at $\kappa = 0$

$$f(t, N) = b^{-2} f(b^y t, bN^{-\theta}) = B^{-2\theta} \bar{f}(B^{y\theta} t, BN^{-1}) \tag{2.19}$$

(with $B = b^{1/\theta}$). We have confirmed this scaling form for $0 \leqslant \kappa < 1$ as shown in the tables. In particular, we read off $1/\nu_\perp = y\theta$ with $y = 1$ for the 2D Ising model and find for the specific heat exponent $\alpha = 2(1 - \theta\nu_\perp) = 0$. We note that this result is different from what would be obtained if the anisotropic hyperscaling relation $2 - \alpha = \nu_\parallel + \nu_\perp$ could be used (as it can in ε-expansion and with averaging over the defect couplings [32]) and would give $\alpha = 1 - 1/\theta$ (for a probably similar situation in the context of directed percolation, see [47, 48]).

2.4. Summary

Numerical studies of the transfer matrix allowed us to find some critical exponents and to guess the finite-size scaling form of the critical spectrum. The tables show the extent by which one can reproduce the expected results, although the lattices needed are quite large. Although our results were obtained in the Hamiltonian limit, by universality (which was explicitly confirmed in a few examples) our results are also correct for the isotropic transfer matrix.

Reconsidering figures 2 and 3, we see that finite-size corrections to the bands are quite small and, furthermore, the bands are θ-independent. This suggests that it might be possible to study at least some types of random systems by investigating a related model with a θ close to 1, which might be easier to deal with.

3. Exact solution of the spectrum

In this section, we calculate exactly the one-particle spectrum Λ_k of the quantum Hamiltonian H (1.6). In particular, we want to prove the results stated in (2.12) and (2.13) for the amplitudes $A^{(Q)}$.

Our starting point is (2.5). In principle, the matrix **M** can be diagonalized by exploiting translation invariance. Then the finite-size dispersion relation is found by the vanishing of a $2\mathcal{M}\times 2\mathcal{M}$ determinant [20]. While this technique works well if $\mathcal{M}$, the number of defects, is finite (and small), in our case $\mathcal{M}\sim N^{1-\theta}$ becomes very large and we need a more efficient approach.

We shall use a technique applied by Flores [49] to the study of a 1D electron gas which is particularly convenient for our purposes. Similar techniques were used for the layered Ising models studied in [1, 3, 4]. We write

$$\mathbf{M}=2\mathbf{I}-\mathbf{R} \tag{3.1}$$

where **I** is the unit matrix and consider the eigenvalue problem of the matrix **R**. Writing out the components, it reads, where for the moment we neglect the boundary terms in (2.1) and (2.5),

$$D_m\psi_{m-1}+V_m\psi_m+D_{m+1}\psi_{m+1}=E\psi_m \tag{3.2}$$

where

$$V_m=\begin{cases}0 & \text{if } m\neq sn\\ V & \text{if } m=sn\end{cases} \tag{3.3}$$

$$D_{m+1}=\begin{cases}1 & \text{if } m\neq sn\\ D & \text{if } m=sn\end{cases} \tag{3.4}$$

where s is an integer and $V=1-\kappa^2$, $D=\kappa$. In the equivalent electron theory [49], V_m is the potential energy of an electron while D_m describes the hopping on a lattice with impurities, as illustrated in figure 4.

The discrete Schrödinger equation (3.2) is written in recursive form

$$\begin{pmatrix}\psi_{m+1}\\ \psi_m\end{pmatrix}=\begin{pmatrix}(E-V_m)/D_{m+1} & -D_m/D_{m+1}\\ 1 & 0\end{pmatrix}\begin{pmatrix}\psi_m\\ \psi_{m-1}\end{pmatrix}. \tag{3.5}$$

Denote $\phi_s:=\psi_{ns+1}$. Then, using (3.5), the wavefunctions at the positions $n(s-1)$, ns and $n(s+1)$ can be related

$$\begin{pmatrix}\phi_s\\ \psi_{ns}\end{pmatrix}=\mathbf{W}(E;n)\begin{pmatrix}\phi_{s-1}\\ \psi_{n(s-1)}\end{pmatrix} \tag{3.6}$$

$$\begin{pmatrix}\phi_{s+1}\\ \psi_{n(s+1)}\end{pmatrix}=\mathbf{W}(E;n)\begin{pmatrix}\phi_s\\ \psi_{ns}\end{pmatrix} \tag{3.7}$$

where the matrix $\mathbf{W}(E;n)$ is given by

$$\mathbf{W}(E;n)=\begin{pmatrix}(E-V)/D & -1/D\\ 1 & 0\end{pmatrix}\begin{pmatrix}E & -1\\ 1 & 0\end{pmatrix}^{n-2}\begin{pmatrix}E & -D\\ 1 & 0\end{pmatrix} \tag{3.8}$$

and we have $\det\mathbf{W}=1$. Inverting (3.6), one obtains by combining with (3.7) a Schrödinger equation for the ϕ_s alone

$$\phi_{s+1}+\phi_{s-1}=\operatorname{tr}\mathbf{W}\phi_s. \tag{3.9}$$

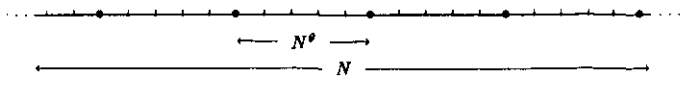

Figure 4. The two different types of sites on the quantum chain.

From the ansatz

$$\phi_s = A\exp(\mathrm{i}Ks) + B\exp(-\mathrm{i}Ks) \tag{3.10}$$

where K is real, we have directly

$$\mathrm{tr}\,\mathbf{W}(E;n) = 2\cos K. \tag{3.11}$$

To calculate tr $\mathbf{W}$, we note that [49], using the definition $E = 2\cos k$,

$$P_n := \begin{pmatrix} E & -1 \\ 1 & 0 \end{pmatrix}^{n-2} = \frac{1}{\sin k}\begin{pmatrix} \sin k(n-1) & -\sin k(n-2) \\ \sin k(n-2) & -\sin k(n-3) \end{pmatrix} \tag{3.12}$$

as can be shown by induction over n. It is now straightforward algebra to obtain the dispersion relation (n even)

$$2\cos K = \frac{1}{\kappa \sin k}[(k^2-1)(1-\cos k)\sin kn + (1+\kappa^2)\sin k\cos kn] \tag{3.13}$$

while, recalling (3.1), the one-fermion energies of the quantum Hamiltonian (1.6) are given by

$$\Lambda_k^2 = 2 - 2\cos k. \tag{3.14}$$

We now discuss the consequences for the spectrum. The Brillouin zone for k is the interval $0 \leqslant k < 2\pi$, which is decomposed in $2n$ bands of size π/n

$$k = \frac{r\pi + \varepsilon}{n} \qquad 0 \leqslant \varepsilon < \pi \qquad r = 0, 1, \ldots, 2n-1 \tag{3.15}$$

where r characterizes the different bands while ε describes the intra-band states. Then the dispersion relation (3.13) becomes

$$2\cos K = \frac{1}{\kappa}\left[(1-\kappa^2)\tan\frac{k}{2}\cos r\pi \sin\varepsilon + (1+\kappa^2)\cos(r\pi+\varepsilon)\right] \tag{3.16}$$

and since for n large and r finite and small, $\tan k/2 \sim 1/n$, this simplifies in the $n \to \infty$ limit to

$$2\cos K = \frac{1+\kappa^2}{\kappa}\cos(r\pi+\varepsilon). \tag{3.17}$$

The levels for which r is small are in any case the only ones with which we can compare our numerical data.

The intra-band states are described by ε

$$\varepsilon = \cos^{-1}\left(\frac{2\kappa}{1+\kappa^2}\frac{\cos K}{\cos r\pi}\right). \tag{3.18}$$

The boundaries of the bands are obtained from the extreme values of ε

$$\varepsilon_\pm = \cos^{-1}\left(\pm\frac{2\kappa}{1+\kappa^2}\right) = \pi(\tfrac{1}{2} \mp \Delta(\kappa)) \tag{3.19}$$

where (2.15) was used. We stress that the band boundaries are independent of r. The lower bound of the band is

$$\Lambda_{\min}^2(r) = 2 - 2\cos\frac{r\pi + \pi(1/2 - \Delta(\kappa))}{n} = \left(\frac{\pi(r+1/2-\Delta(\kappa))}{n}\right)^2 + O(n^{-4}). \tag{3.20}$$

Similarly, the upper bound is found and we have, to leading order in $1/n$,

$$\Lambda_{\min}(r)=\frac{\pi}{n}\left(r+\frac{1}{2}+\Delta(\kappa)\right) \qquad \Lambda_{\max}(r)=\frac{\pi}{n}\left(r+\frac{1}{2}+\Delta(\kappa)\right). \tag{3.21}$$

Finally, we give the energies of the states inside the bands. Up to now, we have not taken into account the boundary conditions, which means that the results derived so far are independent of them. This was already confirmed numerically in section 2. We now recall that periodic boundary conditions in (1.6) imply $\phi_s=\gamma\phi_{s+M}$ with $\gamma=-1$ for $Q=0$ and $\gamma=+1$ for $Q=1$. The quasimomenta for the intra-band states are now discretized

$$K_m=2\pi m/N^{1-\theta}. \tag{3.22}$$

For $\gamma=1$, m is an integer. Thus the intra-band energies are, independently of r,

$$\varepsilon_m=\cos^{-1}\left(\frac{2\kappa}{1+\kappa^2}\cos 2\pi m/N^{1-\theta}\right). \tag{3.23}$$

It is thus sufficient to treat the case $r=0$ and we then find, for m finite and $N\to\infty$,

$$\begin{aligned}\Lambda^2(0,m)-\Lambda^2(0,0)&=2\cos\varepsilon_m/n-2\cos\varepsilon_0/n\\&\simeq\frac{(\pi)^2}{n^2N^{2-2\theta}}\left[m^2 2(1/2-\Delta(\kappa))2\pi\frac{2\kappa}{1-\kappa^2}\right].\end{aligned} \tag{3.24}$$

For $\gamma=-1$, replace m by $m+1/2$. Collecting all results, we have the one-particle amplitudes $A^{(Q)}$ as given in (2.12) and (2.13), including the stated degeneracies.

4. Conclusions

We have obtained exactly the (low-lying) spectrum of a class of layered Ising models which interpolate between the homogeneous system and the McCoy–Wu model. The critical point is not isotropic; rather, the critical exponents are seen to be direction dependent.

The transfer matrix spectrum can be decomposed into two parts: the bands for the one-particle energies and the intra-band levels. As we have shown by using an analogy with an electron gas, one can effectively treat these two subsystems separately. The first one corresponds to an effective subsystem of size $n\sim N^{\theta}$, thereby treating a whole band as a single entity. Its energy levels are equidistant and one could cast the bands *as a whole* into the framework known from conformal invariance.

The long-range behaviour is, however, dominated by the second subsystem, of effective size $\mathcal{M}\sim N^{1-\theta}$. This describes the intra-band excitations, which are given by an effective quadratic dispersion relation. It is exclusively this subsystem whose spectrum should be compared with the transfer matrix spectra of other directed models. The spectrum of this second subsystem is equivalent to that of the tight-binding model [35]. This is probably not very surprising, since both models can be expressed by fermionic harmonic oscillators.

It remains to be seen if the equidistant level spacing of the first subsystem is more than a mathematical curiosity.

Acknowledgments

We thank J C Flores, M Droz, A Patkós and H Herrmann for discussions. One of us (MH) thanks the HLRZ at the KFA Jülich for warm hospitality. We acknowledge useful comments from the referees.

References

[1] McCoy B M and Wu T T 1968 *Phys. Rev.* **176** 631
[2] McCoy B M and Wu T T 1973 *The two-dimensional Ising Model* (Cambridge, MA: Harvard University Press)
[3] Au-Yang H and McCoy B M 1974 *Phys. Rev.* B **10** 886
[4] Wolff W F, Hoever P and Zittartz J 1981 *Z. Phys.* B **42** 259
[5] Hoever P and Zittartz J 1981 *Z. Phys.* B **44** 129
[6] Berche B and Turban L 1991 *J. Phys. A: Math. Gen.* **24** 245
[7] Bariev R 1979 *Sov. Phys.-JETP* **50** 613
[8] McCoy B M and Perk J H H 1980 *Phys. Rev. Lett.* **44** 840
[9] Cabrera G G and Jullien R 1986 *Phys. Rev. Lett.* **57** 3297
[10] Barber M N and Cates M E 1987 *Phys. Rev.* B **36** 2024
[11] Abraham D B, Ko L F and Švrakić N M 1988 *Phys. Rev. Lett.* **61** 2393
[12] Cabrera G G 1990 *Int. J. Mod. Phys.* B **4** 1671
[13] Cardy J L 1984 *J. Phys. A: Math. Gen.* **17** L385
[14] Turban L 1985 *J. Phys. A: Math. Gen.* **18** L325
[15] Peschel I and Schotte K D 1984 *Z. Phys.* **54** 305
[16] Guimarães L G and Drugowich de Felicio J R 1986 *J. Phys. A: Math. Gen.* **19** L341
[17] Henkel M and Patkós A 1987 *J. Phys. A: Math. Gen.* **20** 2199
[18] Henkel M and Patkós A 1987 *Nucl. Phys.* B **285** [FS19] 29
[19] Henkel M and Patkós A 1988 *J. Phys. A: Math. Gen.* **21** L231
[20] Henkel M, Patkós A and Schlottmann M 1989 *Nucl. Phys.* B **314** 609
[21] Baake M, Chaselon P and Schlottmann M 1989 *Nucl. Phys.* B **314** 625
[22] Hinrichsen H 1990 *Nucl. Phys.* B **336** 377
[23] Irving A C, Ódor G and Patkós A 1989 *J. Phys.* A **22** 4665
[24] Grimm U 1990 *Nucl. Phys.* B **340** 633
[25] Hilhorst H J and van Leeuven J M J 1981 *Phys. Rev. Lett.* **47** 1188
[26] Bariev R Z 1990 *J. Phys.* A **22** L397
[27] Burkhardt T W and Igloi F 1990 *J. Phys. A: Math. Gen.* **23** L633
[28] Berche B and Turban L 1990 *J. Phys. A: Math. Gen.* **23** 3029
[29] Igloi F, Berche B and Turban L 1990 *Phys. Rev. Lett.* **65** 1773
[30] Turban L *Preprint*
[31] Bariev R Z and Peschel I *Preprint*
[32] Boyanovsky D and Cardy J L 1982 *Phys. Rev.* B **26** 154
[33] Cardy J L 1990 *Fields, Strings and Critical Phenomena (Les Houches XLIX)* ed E Brézin and J Zinn-Justin (Amsterdam: North-Holland) p 169
[34] Henkel M 1990 *Finite-size Scaling and Numerical Simulation of Statistical Systems* ed V Privman (Singapore: World Scientific) ch VIII, p 353
[35] Henkel M and Herrmann H J 1990 *J. Phys. A: Math. Gen.* **23** 3719
[36] Brower R C, Furman M A and Moshe M 1978 *Phys. Lett.* **76B** 213
[37] Bulirsch R and Stoer J 1964 *Num. Math.* **6** 413
[38] Henkel M and Schütz G 1988 *J. Phys. A: Math. Gen.* **21** 2617
[39] Guttmann A J 1990 *Phase Transitions and Critical Phenomena* vol 13, ed C Domb and J Lebowitz (New York: Academic) p 1
[40] Weniger E J 1989 *Comput. Phys. Rep.* **10** 189

[41] Lieb E, Schultz T and Mattis D 1961 *Ann. Phys.* **16** 407
[42] Domany E and Schaub B 1984 *Phys. Rev.* B **29** 4095
[43] Privman V and Fisher M E 1984 *Phys. Rev.* B **30** 322
[44] Katsura S 1962 *Phys. Rev.* **127** 1508
[45] Barouch E and McCoy B M 1971 *Phys. Rev.* A **3** 786
[46] Henkel M 1987 *J. Phys. A: Math. Gen.* **20** 995
[47] Henkel M and Privman V 1990 *Phys. Rev. Lett.* **65** 1777
[48] Henkel M and Privman V 1991 *Mod. Phys. Lett.* B **5** 555
[49] Flores J C 1991 *Preprint* Geneva